Published in : Physica Status Solidi B. Basic Research (2001), vol. 228, iss. 2, pp. 385-389.
Authors : N. D. Nguyen, M. Germain, M. Schmeits, B. Schineller, and M. Heuken
Status : Postprint (Author's version)

Investigation of Defect Levels in Mg-Doped GaN Schottky Structures by Thermal Admittance Spectroscopy

N. D. NGUYEN (a), M. GERMAIN (a), M. SCHMEITS (a), B. SCHINELLER (b), and M. HEUKEN (b, c)

(a) Institut de Physique, Université de Liège, B5, B-4000 Liège, Belgium

(b) AIXTRON AG, Kackerstr. 15-17, D-52072 Aachen, Germany

(c) Institut für Halbleitertechnik, RWTH Aachen, Templergraben 55, D-52056 Aachen, Germany

Schottky structures based on Mg-doped GaN layers grown by metalorganic chemical vapor deposition (MOCVD) on sapphire substrate are studied by thermal admittance spectroscopy from 90 K to room temperature. Evidence of two impurity levels results from the analysis of the observed peaks in the conductance curves, whose positions and strengths are temperature dependent. The experimental results are analyzed within a detailed theoretical study of the steady-state and small-signal electrical characteristics of the structure. Numerical simulations are based on the solution of the basic semiconductor equations for the structure consisting of two Schottky diodes connected back-to-back by a conduction channel formed by the GaN layer.

Introduction

Successful Mg-doping of GaN has led to a breakthrough in the use of this wide band-gap compound semiconductor both for optoelectronics and for high-power, high-frequency electronic devices. As Schottky-type junctions are the building blocks of these devices, we have performed a thorough analysis of the conduction mechanism in GaN : Mg double Schottky structures. We use numerical simulation to fully explain the experimental results obtained by thermal admittance spectroscopy. It is shown that, due to the simultaneous role of Mg both as a dopant and as a deep impurity, the classical analysis of the Arrhenius plot underestimates the defect ionization energy. Moreover, we show the existence of a second shallow acceptor state with an activation energy of several tens of meV.

Experimental Results

Epitaxial growth by metalorganic chemical vapor deposition (MOCVD) of the GaN layers studied in this work has been detailed elsewhere [1]. The structures consist of a nucleation layer grown directly on top of the sapphire substrate, followed by a 1 µm thick undoped buffer layer and a 2 µm thick Mg-doped layer. Coplanar metallic contacts (Ni/Au) of 0.5 mm diameter and separated by 2 mm, were evaporated on top of the layers.

In Fig. 1, frequency responses of the conductance G divided by $\omega = 2\pi f$, where f is the measurement frequency, of a typical sample, are shown for temperatures ranging from room temperature (RT) down to 90 K. Between RT and 200 K, the G/ω curves show a large peak at the cutoff frequencies f_c in C-f curves (not shown here). The amplitude of this peak decreases as the temperature is lowered. At around 200 K, a shoulder emerges from the high-frequency side of the mentioned peak and is resolved into another peak for temperatures below 170 K. Its position is also temperature dependent.

Published in : Physica Status Solidi B. Basic Research (2001), vol. 228, iss. 2, pp. 385-389.
Authors : N. D. Nguyen, M. Germain, M. Schmeits, B. Schineller, and M. Heuken
Status : Postprint (Author's version)

Fig. 1. *Experimental curves of conductance G divided by $\omega = 2\pi f$ as function of frequency f for temperatures ranging from a) 293 (RT) to 210 K and b) 190 to 90 K (curves from top to bottom)*

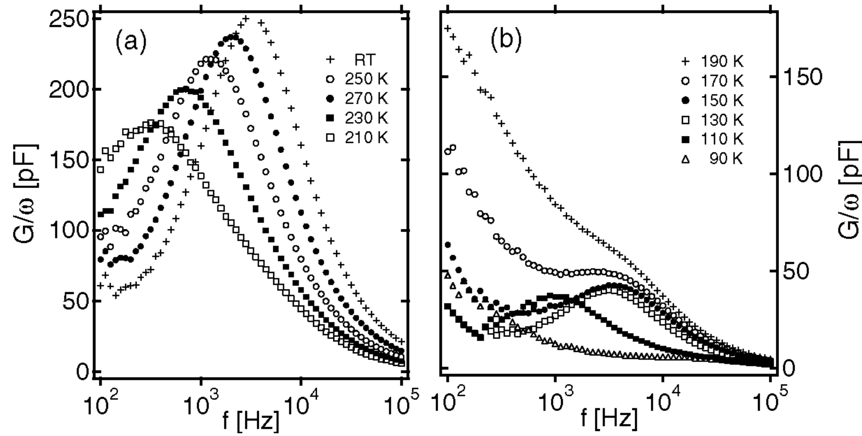

Numerical Simulation

It is known that Mg gives rise to an acceptor-type energy level in the GaN bandgap. Values ranging from 100 to 250 meV above the valence band edge E_V are reported [2-6]. We denote by E_{tA} and N_{tA} the energy position and the total concentration of the level corresponding to the acceptor Mg impurity. In the same way, we introduce E_{tB} and N_{tB}, the energy position and the total concentration of the acceptor level whose existence is suggested by the experimental characteristics at low temperature. To investigate their role in the electrical characteristics of the Schottky diodes, explicit inclusion of the related active population in the semiconductor equations is necessary [7].

The classical basic semiconductor equations are solved numerically in order to obtain as function of the one-dimensional x-coordinate, the hole concentration p, and the occupied level concentrations n_{tA} and n_{tB} which are, with the electrical potential, the primary unknowns involved in the as-formulated system of equations. After solving the latter for the steady-state conditions, the small-signal amplitudes resulting from the application of an ac voltage of frequency $f = \omega/2\pi$ are calculated. A fixed Schottky barrier height $q\varphi_b$, which is chosen identical for both contacts, is imposed in the expression of the boundary conditions. As a result of the ac calculation, the total current density, composed of the hole current density and the displacement current, is obtained. In a final step, we determine the conductance G and the capacitance C from the complex admittance $Y = G + i\omega C$ [7]. Further physical parameters are necessary to effectively reproduce the experimental admittance curves. In addition to $q\varphi_b$, E_{tA} and E_{tB}, N_{tA} and N_{tB}, which have already been introduced, one needs the values of the defect thermal capture cross sections, Σ_A and Σ_B. The hole effective mass is taken as $m_h = 0.8m_0$. The value of the hole mobility μ_h is fixed at 10 cm^2/Vs above $T_0 = 150$ K and given a $(T/T_0)^a$ dependence below that temperature, with α being a free parameter. This T-dependence reproduces the decrease of μ_h with temperature which has been observed experimentally [4]. In order to reproduce with a one-dimensional formalism the electrical characteristics of a structure which is three-dimensional by nature, we have introduced a geometrical parameter R_μ multiplying the carrier mobilities and whose value is of the order of the ratio between the GaN layer thickness, which is in the micrometer range, and the contact diameter, which is in the millimeter range.

Discussion

With the numerical procedure explained above, the electrical characteristics can be calculated at various temperatures, starting from an initial guess for the free parameters. A least-square fit procedure, based on the comparison of the electrical characteristics obtained from the numerical calculation to the experimental data, is used to determine the best values of the parameters. This optimization procedure yields the following values: $(E_{tA} - E_V) = 210$ meV, $(E_{tB} - E_V) = 30$ meV, $N_{tA} = 1 \times 10^{19}$ cm^{-3}, $N_{tB} = 2 \times 10^{16}$ cm^{-3}, $\sigma_A = 2 \times 10^{-19}$ cm^2, $\sigma_B = 2 \times 10^{-19}$ cm^2, $q\varphi_b = 1.05$ eV, $R_\mu = 0.007$, and $\alpha = 3$. The resulting G/ω curves for six temperatures are shown in Fig. 2a. The as-obtained values of the parameters are comparable to those found in the literature for the Schottky barrier height [8, 9] in Au-Ni/p-GaN contacts, the activation energy of the Mg-related acceptor level determined by admittance spectroscopy [2, 3] or by Hall measurements [3, 4], and the thermal capture cross section of the defect A level [3]. The small values obtained for the activation energy and the total concentration of the defect B level, combined with the fact that its effect only appears below 150 K with a weaker amplitude than for level A, may greatly reduce the possibility to easily detect such a level. Nevertheless, more than one acceptor level has been observed in experimental works [2].

Published in : Physica Status Solidi B. Basic Research (2001), vol. 228, iss. 2, pp. 385-389.
Authors : N. D. Nguyen, M. Germain, M. Schmeits, B. Schineller, and M. Heuken
Status : Postprint (Author's version)

Fig. 2. *a) Theoretical G/ω curves as function of frequency for temperatures between RT and 90 K. b) to g) Theoretical capacitance C (dashed lines) and conductance G/ω (dotted lines) curves for the short diode (SD) case, and calculated capacitance C (dash-dotted lines) and conductance G/ω (full lines) curves for the long diode (LD) case. Results are shown for temperatures between 350 and 100 K. The curves are magnified for temperatures of 150 K (× 2) and 100 K (× 10). Positions of the cutoff frequencies f_c and of the defect transition frequencies f_{tA} and f_{tB} are shown for some G/ω curves*

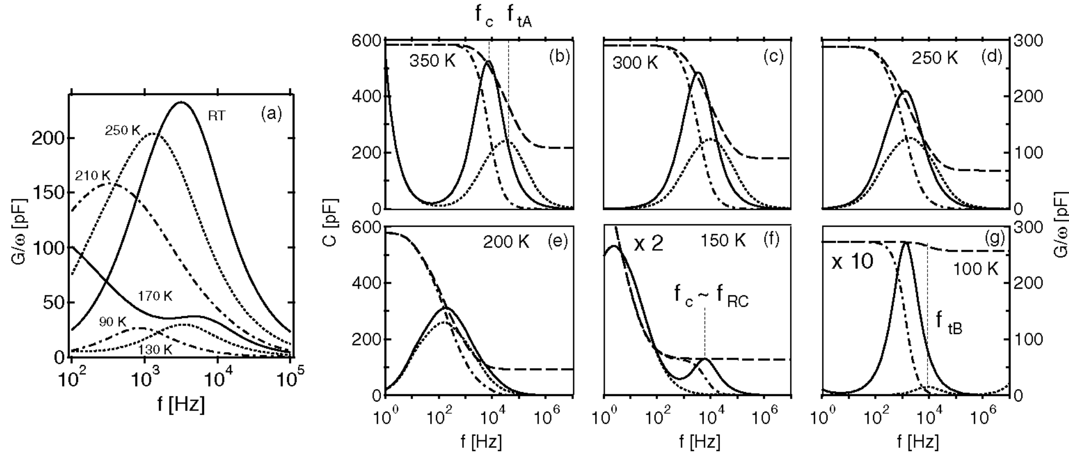

In Figs. 2b to g, we show the calculated capacitance and conductance (G/ω) curves of two different structure types between 350 and 100 K. One (labeled LD, for "long diode") is the complete double Schottky diode structure which has been studied up to now. The other one is essentially the same structure but with a total length of 1 µm and $R_\mu = 1$ (labeled SD, for "short diode"). In this case, series resistance effects, which are explained below, are expected to play no role. The electrical characteristics for temperatures above 200 K are first discussed. In Figs. 2b, c, d and e, the cutoff frequency in the capacitance curve and the peak in the G/ω curve for the SD case are the signature of the Mg-related defect whose transition frequency is denoted by f_{tA}. Starting with this observation, we found that for $T > 240$ K, the cutoff frequency f_c in the LD case is mainly due to an electrical cutoff mechanism, i.e. $f_c \approx f_{RC}$, with $f_{RC} = 1/(2\pi R_S C)$, where R_S is the series resistance of the structure and C the low-frequency value of the capacitance, while for $T < 240$ K, f_c can be identified with f_{tA}. The cutoff frequency for the LD case is therefore the feature resulting from the combination of two mechanisms which are both present in the 200-350 K temperature range. An Arrhenius plot based on the temperature dependence of the peak position between 200 and 300 K yields activation energies of 176 and 107 meV, respectively, for the SD case and the LD case, which are both distinct from the input value of 210 meV. This is partly explained by the fact that the Mg impurity plays a double role: it acts as a dopant and as a deep impurity. The assumptions leading to the identification of the defect transition frequency with the thermal emission rate are not fulfilled [7, 10], even when resistance effects do not take place, i.e. in the SD case.

Below 200 K, the main peak in G/ω moves below the 100 Hz limit of the measurement equipment. A shoulder appears in the 10^3-10^4 Hz frequency range and leads to a second resolved peak around 4×10^4 Hz for temperatures around 150 K (Fig. 2f). The position of the latter is once more that of a $R_S C$ electrical cutoff whose evolution with temperature is mainly due to the variation of the series resistance R_S. The related cutoff frequency $1/(2\pi R_S C)$ is proportional to the conductivity of the layer and therefore proportional to p and μ_h. The calculated bulk concentration of holes p between 130 and 160 K varies only weakly with temperature, this explains why the displacement of this peak is small in this temperature range. Below 130 K, the displacement of the cutoff frequency is explained by the decrease of p due to the variation of the bulk value of (E_F - E_{tB}), where E_F is the Fermi energy, and by the reduction of μ_h due to various scattering mechanisms. In Fig. 2g, the transition frequency f_{tB} of defect B appears at 10^4 Hz in the admittance curves of the SD case at 100 K.

Conclusion

This work shows that only a complete numerical study allows a correct interpretation of the admittance curves. In particular, it is shown that deducing activation energies from an Arrhenius plot of the cutoff frequencies would lead, in the case of the system we have studied, to an underestimation of the activation energies.

Acknowledgements

Financial support by the Belgian Fonds National de la Recherche Scientifique (Contract No. 9.4565.96F) and by an INTAS grant No. N97-0995 are gratefully acknowledged.

References

[1] N. D. Nguyen, M. Germain, M. Schmeits, R. Evrard, B. Schineller, and M. Heuken, J. Cryst. Growth **230,** 600 (2001).

[2] J. W. Huang, T. F. Kuech, H. Lu, and I. Bhat, Appl. Phys. Lett. **68**, 2392 (1996).

[3] D. J. Kim, D. Y. Ryu, N. A. Bojarczuk, J. Karasinski, S. Guha, S. H. Lee, and J. H. Lee, J. Appl. Phys. **88**, 2564 (2000).

[4] W. Götz, R. S. Kern, C. H. Chen, H. Liu, D. A. Steigerwald, and R. M. Fletcher, Mater. Sci. Eng. B **59**, 211 (1999).

[5] U. Kaufmann, M. Kunzer, M. Maier, H. Obloh, A. Ramakrishnan, B. Santic, and P. Schlotter, Appl. Phys. Lett. **72**, 1326 (1998).

[6] A. K. Viswanath, E. Shin, J. I. Lee, S. Yu, D. Kim, B. Kim, Y. Choi, and C. H. Hong, J. Appl. Phys. **83**, 2272 (1998).

[7] M. Schmeits, N. D. Nguyen, and M. Germain, J. Appl. Phys. 89, 1890 (2001).

[8] E. Monroy, F. Calle, J. L. Pau, F. J. Sanchez, E. Munoz, F. Omnes, B. Beaumont, and P. Gi- bart, J. Appl. Phys. **88**, 2081 (2000).

[9] Z. Z. Bandic, P. M. Bridger, E. C. Piquette, and T. C. McGill, Appl. Phys. Lett. **73**, 3276 (1998).

[10] P. Kozodoy, S. P. DenBaars, and U. K. Mishra, J. Appl. Phys. **87**, 770 (2000).